Journal of Statistical Physics, Vol. 69, Nos. 1/2, 1992

A Numerical Study of Sparse Random Matrices

S. N. Evangelou[1]

Received December 31, 1991; final April 23, 1992

A numerical study is presented for the eigensolution statistics of large $N \times N$ real and symmetric sparse random matrices as a function of the mean number p of nonzero elements per row. The model shows classical percolation and quantum localization transitions at $p_c = 1$ and $p_q > 1$, respectively. In the rigid limit $p = N$ we demonstrate that the averaged density of states follows the Wigner semicircle law and the corresponding nearest energy-level-spacing distribution function $P(S)$ obeys the Wigner surmise. In the very sparse matrix limit $p \ll N$, with $p > p_q$, a singularity $\langle \rho(E) \rangle \propto 1/|E|$ is found as $|E| \to 0$ and exponential tails develop in the high-$|E|$ regions, but the $P(S)$ distribution remains consistent with level repulsion. The localization properties of the model are examined by studying both the eigenvector amplitude and the density fluctuations. The value $p_q \simeq 1.4$ is roughly estimated, in agreement with previous studies of the Anderson transition in dilute Bethe lattices.

KEY WORDS: Sparse random matrix ensemble; Wigner–Dyson statistics; density-of-states singularity; Bethe lattice; quantum percolation.

1. INTRODUCTION

Many problems of both classical and quantum physics have discrete representations in terms of $N \times N$ random matrices and the continuum limit is recovered when the order N of the matrix is large. The matrix elements are independent random variables chosen by a probability distribution and the matrices define a statistical matrix ensemble. From the complete eigensolutions for every member of the ensemble both averages and fluctuations of interesting physical quantities can be computed.

Matrices where the randomness plays an important role were intro-

[1] Research Center of Crete, F.O.R.T.H., Heraklion, P.O. Box 1527, Crete, Greece. Permanent address: Department of Physics, University of Ioannina, Ioannina 45 110, Greece.

0022-4715/92/1000-0361$06.50/0

duced long ago in the context of nuclear physics by Wigner and Dyson.[1–4] They were used to overcome the tremendous difficulties of finding eigensolutions for large many-body Hamiltonians, using, instead, an ensemble of random matrices which do not keep the details but only the symmetry of the original problem. All the matrix elements of the corresponding random matrices are independently distributed Gaussian random variables. The required quantity is the joint probability distribution of all the eigenvalues, so that the original diagonalization is now replaced by a statistical probability distribution problem.

The Wigner–Dyson matrices are classified according to symmetry into three universality classes. The case of real and symmetric random matrices defines the so-called Gaussian orthogonal ensemble (GOE),[3] which is exactly solvable. The averaged density of states (DOS) $\langle \rho(E) \rangle$, which is the probability of finding one energy eigenvalue E, obeys a simple semicircle law.[4] The corresponding DOS fluctuations can be estimated to a first approximation by the nearest-level-spacing S distribution function $P(S)$. The distribution $P(S)$ measures two-eigenvalue correlations and it turns out that the probability of finding two energy levels close to each other is very low. This implies strongly correlated eigenvalues repelling their closest neighbors. Moreover, $P(S)$ is a universal quantity, following the Wigner surmise,[4] which depends only on symmetry and not on the random distribution for the matrix elements used as input parameters. The GOE eigenvector statistics is known[3] to be simply characterized by the squared Gaussian χ^2 distribution law, independent of the distribution of the eigenvalues. Such, constant on average, eigenvector amplitude components are extended (delocalized) in nature.

In solid state and statistical physics many problems are also commonly studied in terms of random matrices. The present work is motivated by the fundamental problem of electronic structure in disordered lattice systems and wave propagation in inhomogeneous media. The corresponding matrix representation is known as the tight-binding random matrix ensemble (TBRME) (see, e.g., ref. 5), which has been widely studied since the realization made by Anderson[6] that eigenvectors may show exponential decay properties due to the presence of disorder. The matrices are realized as a discrete representation of the Schrödinger equation, in a hypercubic lattice of sites, choosing as basis set the conventional local site orbitals $|n\rangle$. The diagonal matrix elements $\langle n| H |n\rangle$ denote the potential ε_n at site $|n\rangle$. The off-diagonal matrix elements $\langle n| H |n'\rangle$ are different from zero only when n and n' are nearest neighbors in the lattice. The nonzero off-diagonal values define the hopping matrix element V, which is proportional to $h^2/2ma^2$, where h is Planck's constant, m is the electron effective mass, and a is the lattice spacing.

The Anderson model[6] arises when the ε_n are random variables while V is a constant setting the energy scale. Then for every realization of the random set ε_n, $n = 1, 2, \ldots, N$, one obtains a member of the corresponding TBRME. In the absence of spin effects the tight-binding random matrices are real and symmetric but clearly of drastically different structure than the GOE. Their differences lie in the fact that they are instead short-ranged and sparse. They have in d dimensions random diagonal matrix elements (diagonal disorder) and d off-diagonal matrix elements per matrix row distributed close to the diagonal, which may also be random variables (off-diagonal disorder); the rest of the matrix elements are identically equal to zero. This specific matrix structure arises, as discussed above, because the matrix elements connecting only the nearest neighbors of every lattice site are different from zero.

The TBRME can be also defined on pseudolattices, such as the Bethe lattice, characterized by a coordination number. The Bethe lattice can roughly approximate real d-dimensional lattices of the same coordination number. This correspondence becomes precise only for the case of infinite coordination, where the Bethe lattice maps onto an infinite-d lattice. Random matrix ensembles more sparse than the TBRME can be obtained by diluting the real or the pseudolattices, that is, by removing sites or bonds at random, leading to a percolating cluster lattice geometry.[7] Then the coordination number, which counts the average number of nearest neighbors for each site or equivalently the average number of nondiagonal elements per matrix row, takes a value lower than d.

The present study focuses on a mean-field case. We consider the $d = \infty$ TBRME where each site is allowed to extend its range not as usual to its nearest neighbors, but to all the other sites. In this limit the $N \times N$ matrices become full, having only nonzero elements, and for appropriate choices for the random distributions[1–4] are precisely the GOE matrices. The sparse random matrices studied in this paper are similar to those obtained from diluting such a $d = \infty$ TBRME. This is equivalent to considering a quantum percolation problem[7] on the $d = \infty$ TBRME or the ∞-coordination dilute Bethe lattice. Such kinds of sparse matrices also appear in a variety of related problems, ranging from dilute spin systems[8] to combinatorial optimization.[9]

We introduce a sparse random matrix ensemble (SRME)[10–14] characterized by a finite mean number p of nonzero elements per row. When $p = N$ the GOE limit is obtained and small p values simulate more realistic finite-d dilute lattice situations. The SRME, apart from being useful in understanding many physical and engineering problems, has a profound interest for the following reasons: First, it allows us to consider the limits of validity of the Wigner–Dyson theories and their universal statistics when

the matrices deviate from GOE. Second, the SRME can be used as a model for considering fluctuation properties of disordered conductors,[15-17] when they depart from the delocalization limit and approach the localization threshold. More important is the fact that the SRME permits the description of a delocalization–localization Anderson transition at a critical value of $p = p_q$. Third, the model can be used for studying the quantum-mechanical behavior of systems that are classically chaotic.[18] The main question in this case is, again, whether the Wigner–Dyson universality remains under these conditions. Finally, an extra reason for considering this model is that it is amenable, up to some extent, to various analytical treatments using the replica and supersymmetric method,[11-14], unlike the original TBRME on 2- and 3-dimensional lattices.

Since the known remarkable analytical solutions for the SRME[11-14] are nevertheless limited in their extent, we chose to study the problem numerically. We are aiming for the independent confirmation of the previous analytical results via an independent method and since our numerical approach does not suffer from the same sorts of limitations, we can answer an even more general set of questions. In the rest of the paper we proceed as follows: The model and the method of calculation can be found in Section 2. In Section 3 we focus on the averaged DOS and in particular demonstrate the appearance of the $\langle \rho(E) \rangle \propto 1/|E|$ singularity as $|E| \to 0$, in the very sparse matrix limit $p \ll N$. The exponential tails in the high-$|E|$ regions can be also seen in this limit. In Section 4 the eigenvalue statistics is considered and we apply a quantitative criterion of localization based on the DOS fluctuations, so that we are able to locate the Anderson transition threshold value p_q. In Section 5 we present results for the level-spacing distribution function $P(S)$ as another important measure of the DOS fluctuations. Moreover, we examine the validity of the GOE universality and present strong evidence that it persists even in the very sparse random matrix limit as long as $p > p_q$. Besides the demonstration of the behavior for the DOS fluctuations, we present results on the corresponding eigenvector amplitude component distributions in Section 6. Finally, we discuss our findings in relation to the Anderson transition in dilute Bethe lattices, in connection with previous studies, and we present our conclusions in Section 7.

2. THE MODEL AND THE METHOD OF CALCULATION

We consider real and symmetric $N \times N$ matrices

$$\mathbf{H} = \sum \sum_{i,j=1}^{N} H_{i,j} |i\rangle\langle j| \tag{1}$$

written in a convenient basis set ($|i\rangle$, $i=1, 2,..., N$). The matrix elements $H_{i,j}(=H_{i,j}^*=H_{j,i})$ are independent, identically distributed random variables chosen from the probability distribution

$$P(H_{i,j})=\left(1-\frac{p}{N}\right)\delta(H_{i,j})+\frac{p}{2N}\left[\delta\left(H_{i,j}-\frac{1}{\sqrt{p}}\right)+\delta\left(H_{i,j}+\frac{1}{\sqrt{p}}\right)\right] \quad (2)$$

The model of Eq. (1) with the distribution from Eq. (2) contains one basic parameter, the "mean connectivity" number p. We start with the GOE when $p=N$ and by lowering p we can study deviations from the GOE. Extensions of the model are obtained if we vary the ratio between the positive and the negative matrix elements, which from Eq. (2) are equal to one on the average. Apart from such asymmetry, we can also introduce a continuous, rather than binary, distribution of the random matrix elements. In the latter case another parameter must be added describing the additional randomness. No qualitative changes in the results reported here were found for such extended SRMEs.

The method of calculation mostly relies on the numerical computation of eigenvalues and eigenvectors in finite samples from the SRME. Our matrix ensemble consists of matrices of sizes extending up to 2000×2000. For the numerical diagonalization it is convenient to employ the usual vectorized diagonalization routines, although the Lanczos algorithm (e.g., ref. 19) is also suitable, by making use of the sparse nature of the matrices. The complete eigensolutions (eigenvalues and eigenvectors) in the whole energy domain are found for a given p value for various N values and a large ensemble was considered. We have also allowed the matrix size N to vary, for a given p, in order to determine the large-N behavior. We mostly focus on the spectral properties of the model and determine the resulting spectral DOS as well the DOS fluctuations. The localization properties of the model require a more detailed study by including the eigenvectors as discussed in Section 6.

The DOS calculation proceeds as follows: We collect all the eigenvalues in energy bins for many different, randomly generated matrices, so that the average $\langle\rho(E)\rangle$ can be determined. The errors arising in the calculations have been estimated and are related to a novel localization criterion as follows: If the mean number of eigenvalues in a given energy bin of width E is $\langle n(E)\rangle$, then it implies a variance $\langle\delta n(E)^2\rangle=\langle n(E)^2\rangle-\langle n(E)\rangle^2$ proportional to the mean $\langle n(E)\rangle$. This is a result of ordinary Poisson statistics, but refers only to localized states. The sample-to-sample DOS fluctuations are instead even smaller for delocalized states as a consequence of the validity of the Wigner–Dyson theory.[1–4] As proposed in ref. 15, we expect $\langle\delta n(E)^2\rangle$ to be much lower than $\langle n(E)\rangle$

for delocalized states, varying logarithmically with $\langle n(E)\rangle$. Therefore, the relative variance $\langle \delta n(E)^2\rangle/\langle n(E)\rangle$ is of order one when the states in the energy bin are localized and much smaller than one and decreasing with $\langle n(E)\rangle$ when they are delocalized. This reasoning is valid when $\langle n(E)\rangle$ is a small number. In fact, it was estimated that for critical states[15] $\langle \delta n(E)^2\rangle$ is also proportional to $\langle n(E)\rangle$, but with a proportionality index of about 1/2. Therefore, no significant statistical error arise for calculations of averaged values in regions of delocalized states as performed in Section 3. The errors become more significant, reaching normal statistical bounds in the localized phase.

Another source of error in our type of calculation arises because of the finite size N for each chosen sample. This results in a limited number of sites in a given energy bin because the average level spacing $\propto 1/N$ is finite. As a consequence, when N is not large enough, the spectrum of eigenvalues shows pronounced discreteness. This kind of error also limits us in extending the calculation down to very small energies. We have also checked convergence of our results by varying the system size. For the system sizes considered we have found a large number of eigenvalues for $|E| \geqslant 0.001$ which were collected in energy bins of width $\Delta E = 0.025$. The above errors have been monitored in our calculations by choosing many random sample matrices and large enough matrix sizes. The total error has been minimized to within a few percent, and our results might be interpreted as refering to the infinite-N limit.

3. THE AVERAGED DOS $\langle \rho(E)\rangle$

The DOS at a particular value of p is symmetric with respect to $E=0$. We introduced the normalization condition $\langle \mathrm{Tr}\, \mathbf{H}^2\rangle = N$, which sets the energy scale, since it requires the second moment of the DOS to be always one. This condition guarantees that the DOS has a compact structure in the region $[-2, 2]$ when $p = N$. For $p \ll N$ the majority of eigenvalues still lie in the same region, but exponential tails develop outside $[-2, 2]$. We report numerical results for the DOS at various p's in Fig. 1. It can be seen that for very high down to moderate p values the Wigner semicircle law

$$\langle \rho(E)\rangle = \frac{1}{\pi}\left(1-\frac{E^2}{4}\right)^{1/2}, \qquad |E| \leqslant 2 \tag{3}$$

holds to a high accuracy. By lowering p even further, down to values corresponding to 2- and 3-dimensional real lattices, we observe two characteristic novel features of the DOS: First, for special energies whose number progressively increases, δ-function peaks are seen. They are special

degenerate states due to the dilute structure of the matrices. A simple explanation for their existence was proposed[20] for quantum percolation models in 2 and 3 dimensions. They occur because of special regions of the self-similar fractal percolating cluster geometry. It must be mentioned that in our case the percolating cluster is defined on an infinitely-coordinated dilute Bethe lattice.

The second and more important observation refers to the continuous component of the spectrum close to the center. For small p values a singularity of the form

$$\langle \rho(E) \rangle \propto \frac{1}{|E| \log(|E|)^3} \qquad \text{as} \quad |E| \to 0 \tag{4}$$

appears. Since the E range where the diverging $\langle \rho(E) \rangle$ occurs is very close to zero and the type of divergence of the DOS is not clearly visible due to the coarse graining procedure involved in Figs. 1b–1d, we choose to plot the averaged integrated density of states (IDOS) against E by including the very small energies. The IDOS is given by the integral over the rhs of the Eq. (4), which is proportional to $(1/\log|E|)^2$. Therefore, in the double

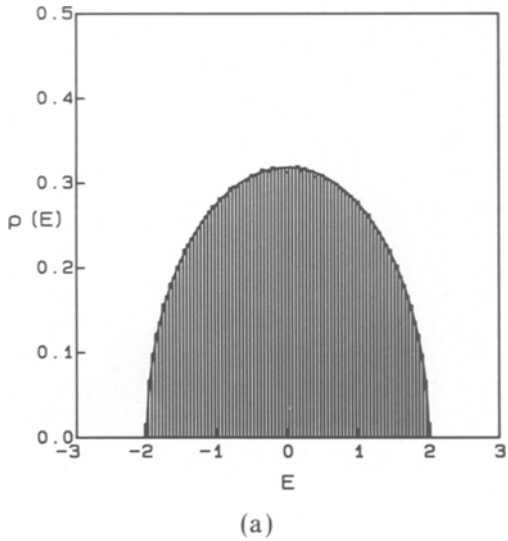

(a)

Fig. 1. Plot of the normalized averaged DOS $\langle \rho(E) \rangle$ together with the Wigner semicircle law for sparse random matrices of $N = 2000$ with four different values of p: (a) $p = N$ from 1000 matrices, (b) $p = 8$ from 200 matrices, (c) $p = 5$ from 100 matrices, (d) $p = 3$ for 100 matrices, and (e) $p = 15$ and $p = 8$ together with the Wigner semicircle law superimposed.

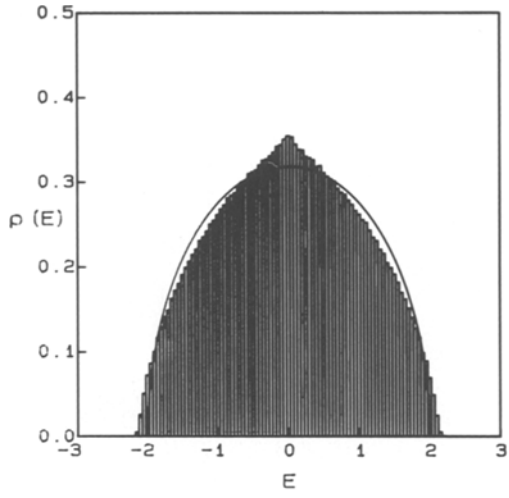

(b)

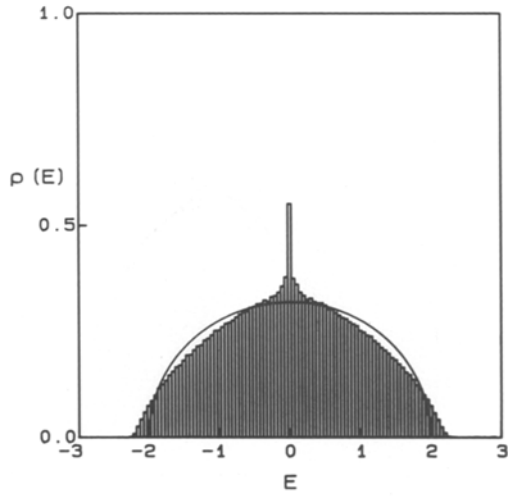

(c)

Fig. 1 (*Continued*)

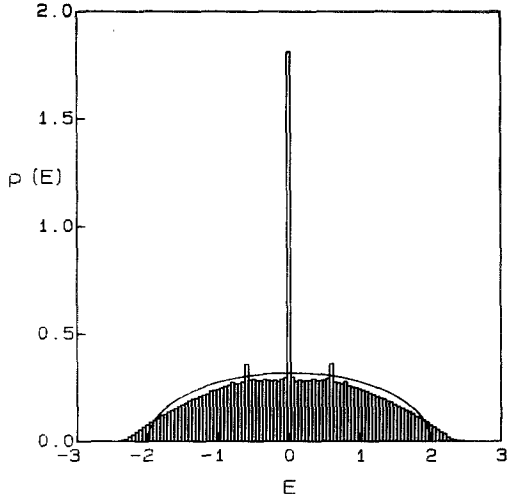

(d)

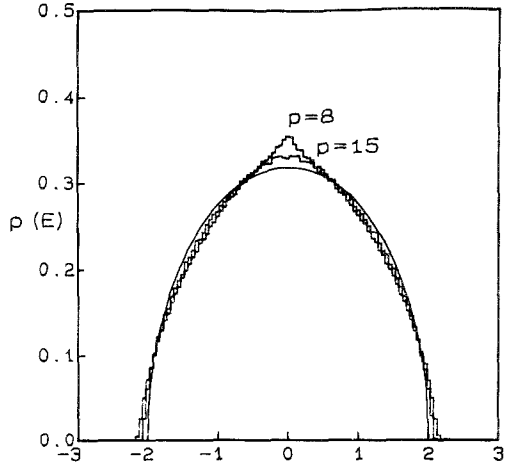

(e)

Fig. 1 (*Continued*)

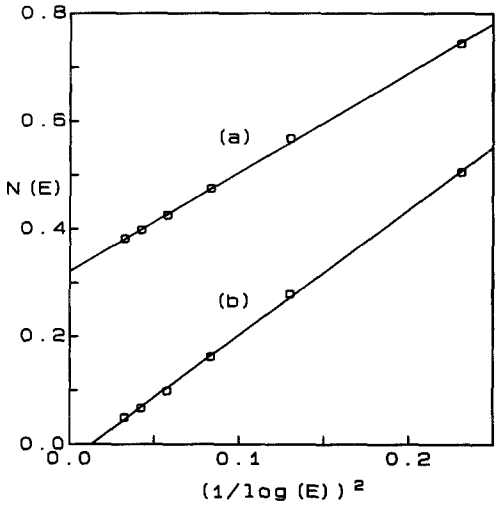

Fig. 2. Plot of the averaged integrated density of states $N(E)$ for E close to $E=0$ for (a) $p=5$ and (b) $p=3$. The straight lines imply that the singularity is of the form of Eq. (4).

logarithmic plot of Fig. 2 the law of Eq. (4) implies that for small p values the data should lie on straight lines. Despite the various sources of error, the data lie rather accurately on straight lines and the peak of the form $\langle \rho(E) \rangle \propto 1/|E|$ is displayed.

From the results of refs. 11–13, where a reduction of the problem to an integral equation was achieved, a power of 2 instead of 3 is expected for the logarithmic part of the singularity. Our data instead correspond precisely to a Dyson singularity.[21] The deviation of our results from the calculations of refs. 11–13, if not genuine, could be also understood as arising from numerical difficulties in our approach due to the very small energy range considered. Such a singular structure for the DOS was previously shown[22] in disordered lattices with the randomness in the off-diagonal matrix elements. In fact the Dyson singularity is a signal of large fluctuations in a random medium and was related to log-normal distributions, $1/f$-noise phenomena,[22] and localization. At values of p close to p_c we see a dip of the DOS near the band center, as in refs. 19 and 20.

4. THE DOS FLUCTUATIONS AND THE QUANTUM PERCOLATION TRANSITION

From Eq. (2) the mean and the variance of the random matrix elements are $\langle H_{i,j} \rangle = 0$ and $\langle H_{i,j}^2 \rangle = 1/N$, respectively. Therefore, the

disorder vanishes in the thermodynamic limit and one might conclude that the SRME belongs to the delocalized phase for any p. However, this is not so, because the underlying percolating geometrical disorder remains, so that classical and quantum percolation transitions are expected. These occur at values $p_c = 1$ and p_q, in general higher than p_c, respectively. The estimate of $p_c = 1$ arises simply from the usual dilute Bethe lattice percolation concentration defined as the inverse connectivity $1/N$.[7] For the SRME when $p \geqslant 1$ an infinite connected cluster appears. A Bethe lattice of connectivity σ studied in ref. 23 allowed a determination of p_q, estimated from the solution of the equation

$$1 + [\sigma^2 p_q]^{-1} = (\sigma p_q)^{2/(\sigma - 1)} \tag{5}$$

For the infinitely coordinated case ($\sigma \to \infty$) it gives the value $p_q \simeq 1.4 p_c$, a bound which implies that for p values below $p_q \simeq 1.4$ all states should become localized. Extimates for the quantum percolation thresholds of finite-connectivity Bethe lattices have also been reported in ref. 19.

In order to establish the p_q value, we use a simple criterion of localization based on the DOS fluctuations. It involves the relative variance ratio $R = \langle \delta n(E)^2 \rangle / \langle n(E) \rangle$, which is studied for various p values. When R is not much smaller than one and does not diminish upon increasing the matrix size the corresponding states must have reached the localization point. Otherwise, the states remain delocalized. This allows a simple criterion of localization to be established simply as $R \geqslant 1/2$.

In Figs. 3a–3d the DOS is displayed together with the relative fluctuations for $p = 1$ to 1.6 by collecting the eigenvalues in specific energy bins. For such small values of p the very dilute structure of the matrices causes the multiple appearance of eigenvalues at many energies. In particular, for $p = p_c = 1$ a dip of the DOS can be seen near the band center. The measure of the relative DOS fluctuations is rather high in this case, denoting localized states. From Figs. 3a–3d a quantum percolation threshold of about 1.4 is found, in agreement with ref. 23.

5. THE LEVEL-SPACING DISTRIBUTION FUNCTION $P(S)$

In order to unravel the localization properties of the model, we have also considered the most common spectral fluctuation measure, the nearest-level-spacing distribution function $P(S)$. For delocalized states the Wigner–Dyson statistics is expected to occur related to a smooth, correlated spectrum exhibiting level repulsion and spectral rigidity. For the localized phase instead the corresponding spectra are uncorrelated and

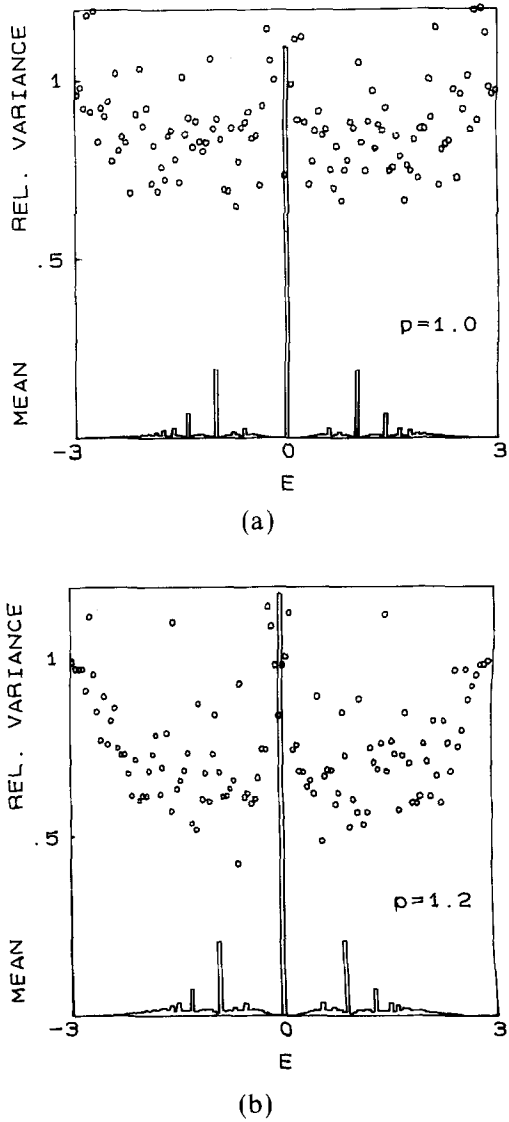

Fig. 3. Plot of a mean DOS and the relative DOS variance R for $N = 1000$ and (a) $p = 1$, (b) $p = 1.2$, (c) $p = 1.4$, (d) $p = 1.6$. When the relative DOS fluctuation R exceeds 1/2 the states become localized.

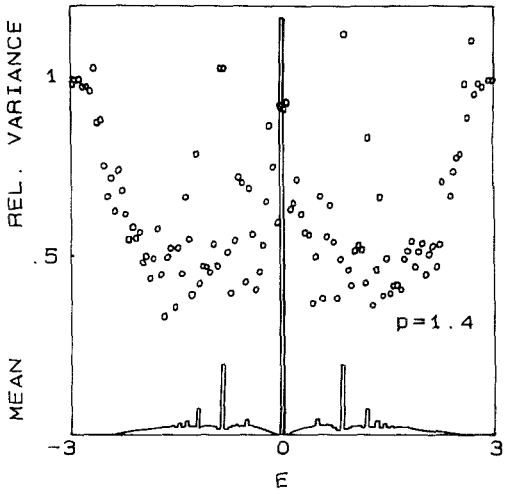

(c)

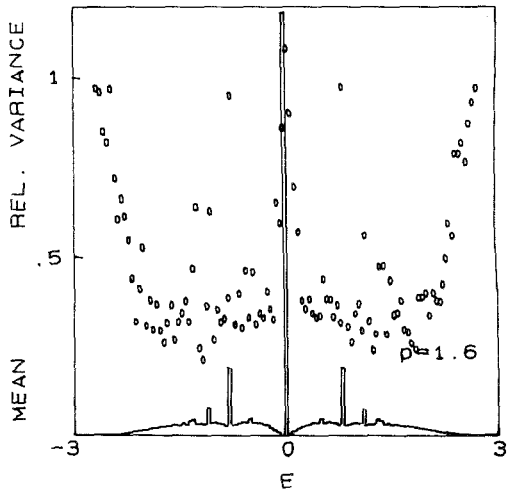

(d)

Fig. 3. (*Continued*)

should obey normal statistics. For $P(S)$ this implies the law of the well-known Wigner surmise,

$$P(S) = (\pi S/2) \exp(-\pi S^2/4) \tag{6}$$

for delocalized states, normalized so that the average level spacing is one. For localized states instead $P(S)$ should cross over to the usual Poisson law[24]

$$P(S) = \exp(-S). \tag{7}$$

We have studied the distribution function $P(S)$ of the nearest-energy-level spacings $S_n = E_{n+1} - E_n$ for various p values. The calculations are done by obtaining the eigenvalues for many random runs, their total number being approximately 50,000, and subsequently by deconvoluting the spectrum,[17] in order to retain a constant DOS. This is equivalent to studying the distribution of the difference

$$\langle \mathcal{N}(E_{n+1}) \rangle - \langle \mathcal{N}(E_n) \rangle = (E_{n+1} - E_n) \frac{\partial}{\partial E} \langle \mathcal{N}(E) \rangle$$

where $\langle \mathcal{N}(E) \rangle$ is the averaged IDOS at energy E. The result for a very small value of $p = 3$ is displayed in Fig. 4, shown to agree perfectly well

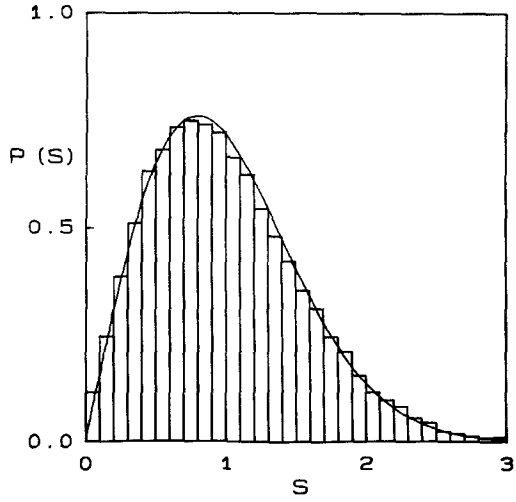

Fig. 4. The calculated level-spacing distribution function for $N = 1000$ and $p = 3$. The data are in histogram form for 100 random matrices and cover the full energy range. The horizontal line is in units of the local mean-level spacing and the solid curve is the Wigner surmise, Eq. (6).

with the corresponding Wigner surmise, Eq. (6). In ref. 10, a crossover to a Poisson law was found for p values below the critical concentration p_q. The remarkable result of this section is the perfect validity of the Wigner–Dyson universality even when one is largely deviating from the GOE limit.

6. THE EIGENVECTOR AMPLITUDE FLUCTUATIONS

In order to probe the localization properties of the model, we have also considered the corresponding eigenvectors. Their delocalized nature is clearly seen to remain down to small p values, as long as $p \geqslant p_q$. The delocalized eigenvector amplitude distributions shown in Fig. 5 for $p = 3$ are also likely to display multifractal scaling, as was previously observed in a related banded random matrix ensemble (BRME).[25,26] It must be pointed out, however, that the SRME is strictly different from the BRME proposed in ref. 26. In the $N = \infty$ limit the BRME always has localized states and no Anderson transition is expected to occur if the range of nonzero matrix elements is shorter than N.

In order to determine the extent of localization, we have also considered a very common localization measure: This is the inverse participation ratio ($IPR^{(i)}$) for the energy eigenvalue E_i, defined as

$$IPR^{(i)} = \sum_{j=1}^{N} \psi_j^{(i)4} \tag{8}$$

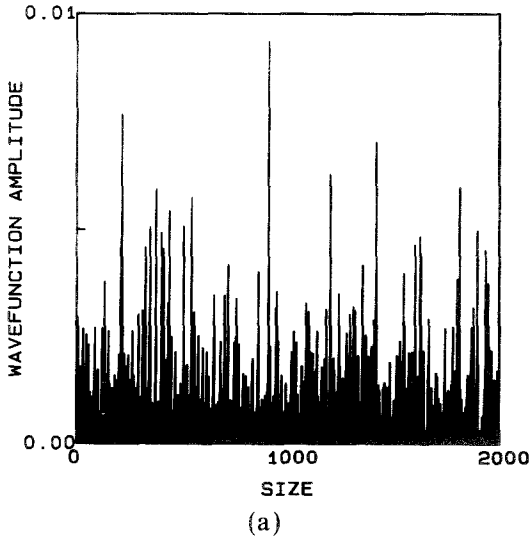

Fig. 5. Plot of a particular eigenvector amplitude for $N = 2000$ and $p = 3$ for different spatial regions in order to display its random self-similar character.

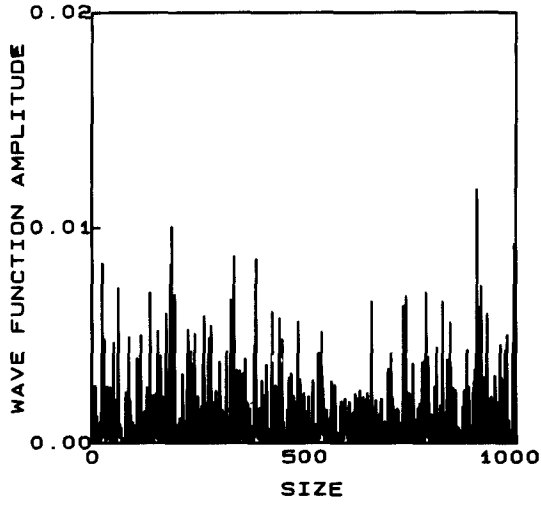

(b)

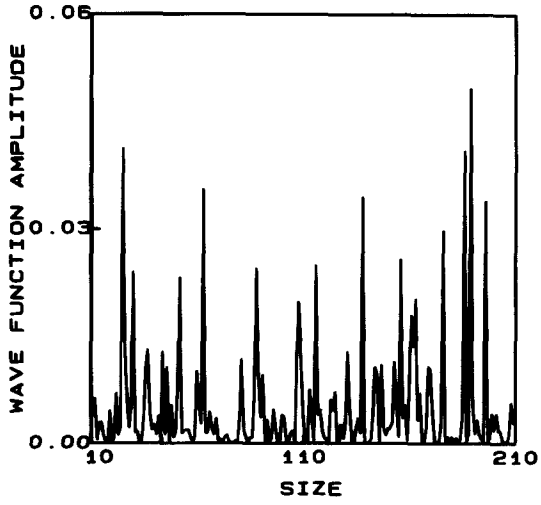

(c)

Fig. 5. (*Continued*)

where $\psi_j^{(i)}$, $j = 1, 2, ..., N$, are the corresponding eigenvector components. The *IPR* should somehow count the inverse of the number of sites where the amplitude is concentrated. Therefore, for very delocalized states it should be very low, proportional to $1/N$, approaching one only in the opposite limit of extreme localization. Moreover, it is known that *IPR* is a wildly fluctuating measure, especially close to the localization transition.

In Figs. 6 and 7 the IPR is shown for various p values for two matrix sizes. It can be seen that for low $p < p_q$ the eigenvectors have small localization lengths, being localized in less than about $\sqrt{N}$ sites. The straight vertical lines in Figs. 6a–6c denote the special localized states due to the percolating cluster geometry discussed in Section 3. For higher $p \gg p_q$ the eigenvectors displayed in Figs. 6d and 6e become delocalized. It is worth pointing out two facts: First, for the results with the larger N shown in Fig. 7 it is seen that for delocalized eigenstates ($p > p_q$) the *IPR* fluctuations diminish while they remain significant only for localized states ($p < p_q$). The second observation refers to Figs. 6d and 7c, where near the center of the spectrum eigenvectors with shorter localization lengths are seen (larger *IPR*), as normally happens close to the spectral edges. The spectral region where this occurs corresponds to the $1/E$-singularity peak, which is therefore associated with states with shorter localization lengths.

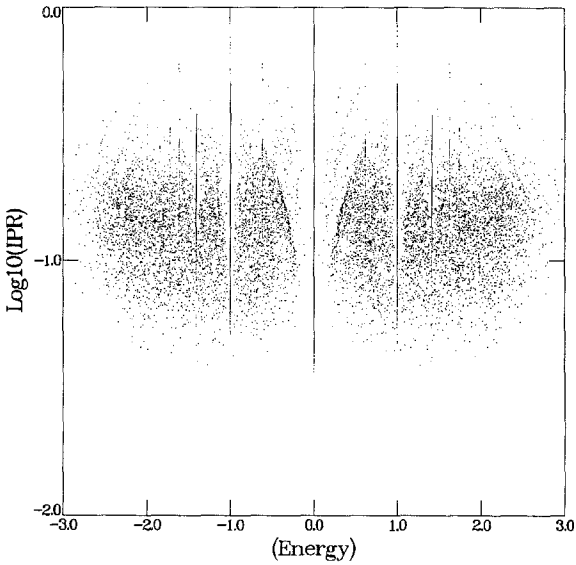

(a)

Fig. 6. Plot of the *IPR* versus energy for $N = 100$ and 500 random matrices: (a) $p = 1$, (b) $p = 1.4$, (c) $p = 1.6$, (d) $p = 5$, (e) $p = N$.

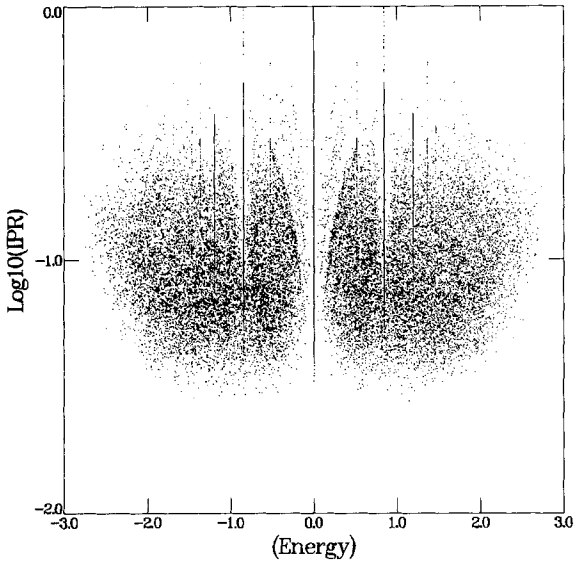

(b)

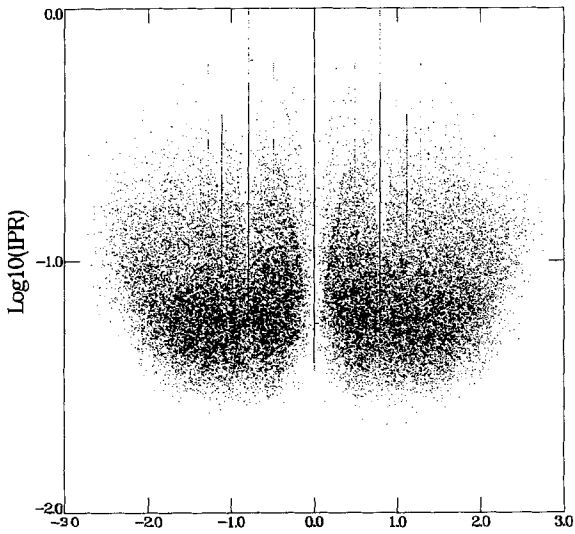

(c)

Fig. 6. (*Continued*)

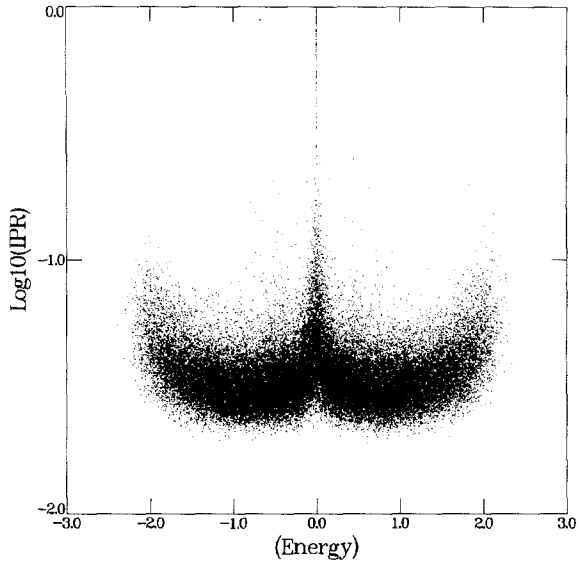

(d)

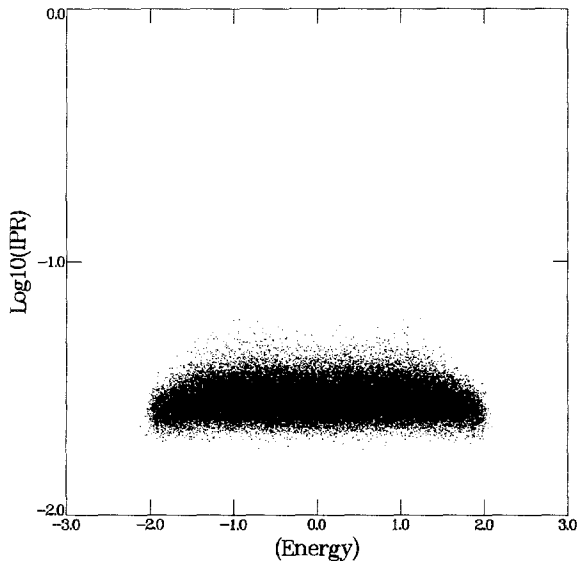

(e)

Fig. 6. (*Continued*)

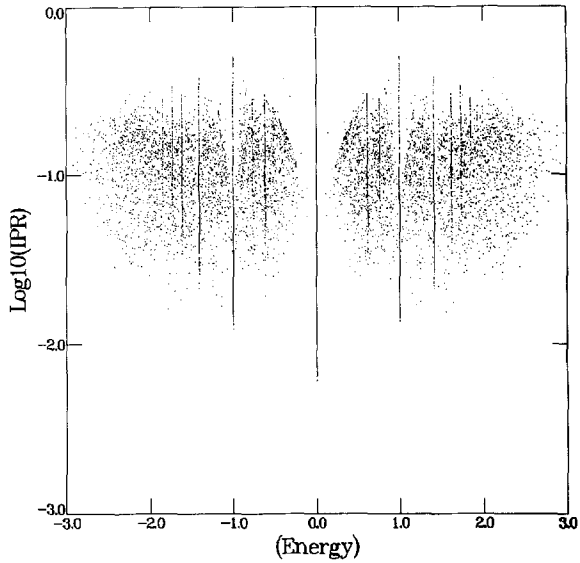

(a)

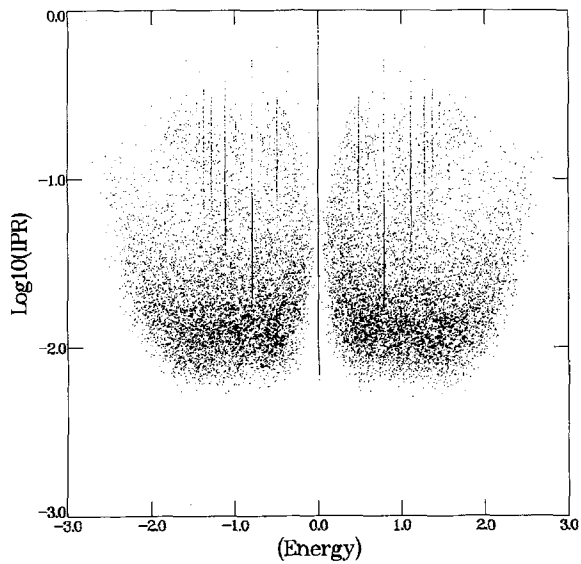

(b)

Fig. 7. Plot of the *IPR* versus energy for $N = 1000$ and 25 random matrices: (a) $p = 1$, (b) $p = 1.6$, (c) $p = 5$, (d) $p = N$.

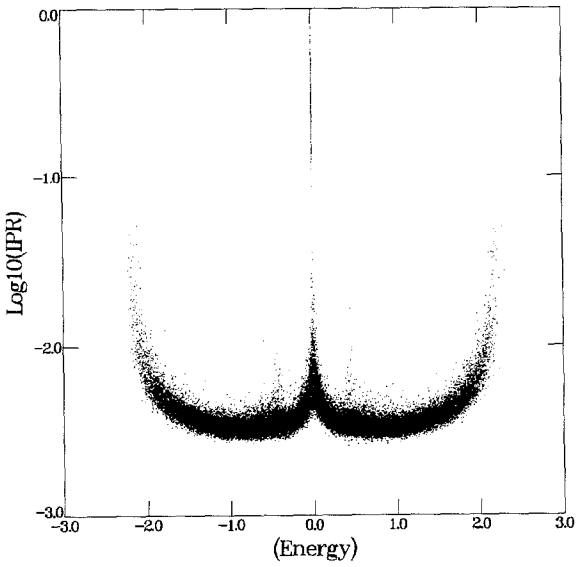

(c)

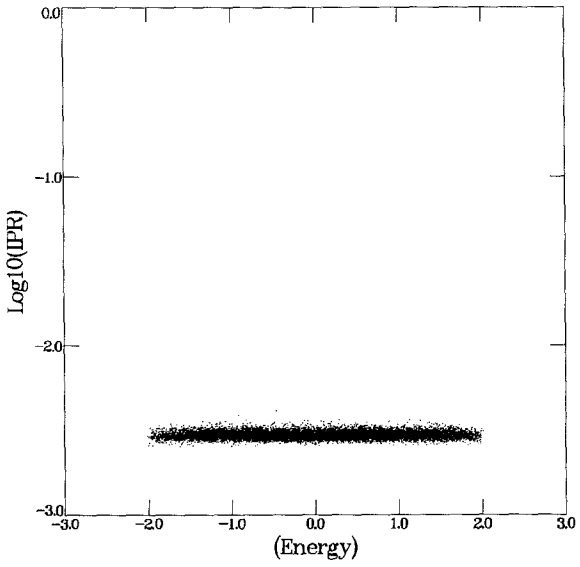

(d)

Fig. 7. (*Continued*)

7. DISCUSSION

The Anderson localization phenomenon implies a drastic departure not only from the conventional Bloch theory of periodic modulated eigenvector amplitudes in nonrandom matrices, but also from the constant on average but fluctuating eigenvector amplitudes in the Gaussian matrix ensembles. The latter correspond to high-coordination number or high-dimensionality lattice systems where no localization is expected. As a consequence of this fact, the Wigner surmise and the level repulsion for the eigenvalue fluctuations associated with the GOE is naturally expected to characterize the delocalized parts of a spectrum in the presence of disorder. This analogy has been quite rigorous and has been exploited for responsability of the mesoscopic physics fluctuation phenomena in small metallic systems.[15] On the other hand, for disordered systems of very small coordination number or low dimensionality it is known that localized states should exist and the level spacings must be distributed according to a Poisson law, which permits clustering of eigenvalues.[24] From these observations it follows that from the spectral fluctuation properties of disordered systems alone we can distinguish between delocalized and localized states.

Results along these lines are reported in this paper for an SRME when the coordination number p is allowed to vary. We have studied the problem for a range of values of the mean matrix row concentration p starting from the GOE limit $p = N$ down to the very dilute percolation limit ($p = 1$). For p much smaller than N we see that the states are unusually fluctuating when compared to the GOE states, since we are entering into the localization regime. We have also been able to locate the Anderson transition, where a drastic change of behavior occurs at a value p_q. The main results are as follows: (i) The DOS satisfies perfectly the semicircle law from $p = N$ down to moderate values of p, and a crossover to a DOS with a $1/|E|$-singularity peak for $|E|$ near zero is seen by lowering p significantly. (ii) The nearest-level-statistics distribution is very close to the Wigner-surmise law for $p > p_q$. Results (i) and (ii) signify the importance of the Wigner–Dyson theory, even when drastically departing from the GOE. (iii) A simple criterion based on the DOS fluctuations allows p_q to be evaluated, in agreement with previous estimates. (iv) Finally, the eigenvector amplitudes are studied and seen to have strong fluctuation properties when approaching localization.

The prospects for future studies of the SRME lie on two fronts: The first is its extension in order to include other universality classes, e.g., by brakeing the time-reversal invariance. The second is the application of the model for exploration of the critical behavior, also in connection with the possibility of constructing a mean-field theory of Anderson localization.

ACKNOWLEDGMENTS

This work was supported in part by EEC, contract SCC*-CT90-0020, and also a PENED Research Grant of the Greek Secretariat of Science and Technology.

REFERENCES

1. E. P. Wigner, *Ann. Math.* **62**:548 (1955); **65**:203 (1957).
2. F. Dyson, *J. Math. Phys.* **3**:140 (1962); **3**:1199 (1962).
3. C. E. Porter, *Statistical Theories of Spectra: Fluctuations* (Academic Press, New York, 1965).
4. M. L. Mehta, *Random Matrices and the Statistical Theory of Energy Levels* (Academic Press, New York, 1967).
5. E. N. Economou, *Green's Functions in Quantum Physics* (Springer, New York, 1983).
6. P. W. Anderson, *Phys. Rev.* **109**:1492 (1958).
7. D. Stauffer, *Introduction to Percolation Theory* (Taylor and Francis, London, 1985); see also D. Stauffer and A. Aharony, *Introduction to Percolation Theory*, 2nd ed. (1992).
8. R. B. Griffiths, *Phys. Rev. Lett.* **23**:17 (1969).
9. J. R. Banavar, D. Sherrington, and N. Sourlas, *J. Phys. A* **20**:L1 (1987); M. Mezard and G. Parisi, *J. Phys. Lett.* (Paris) **46**:L771 (1985).
10. S. N. Evangelou and E. N. Economou, *Phys. Rev. Lett.* **68**:361 (1992).
11. G. J. Rodgers and A. J. Bray, *Phys. Rev. B* **37**:3557 (1988).
12. G. J. Rodgers and C. De Dominicis, *J. Phys. A* **23**:1567 (1990).
13. A. D. Mirlin and Y. V. Fyodorov, *J. Phys. A* **24**:2273 (1991).
14. Y. V. Fyodorov and A. D. Mirlin, *Phys. Rev. Lett.* **67**:2049 (1991).
15. B. L. Al'tshuler, I. Kh. Zharekeshev, S. A. Kotochigova, and B. I. Shklovskii, *Sov. Phys. JETP* **67**:625 (1988).
16. Y. Imry, *Europhysics Lett.* **1**:249 (1986).
17. S. N. Evangelou, *Phys. Rev. B* **39**:12895 (1989).
18. F. Haake, *Quantum Signatures of Chaos* (Springer, Berlin, 1991).
19. S. N. Evangelou, *Phys. Rev. B* **27**:1397 (1983).
20. S. Kirkpatrick and T. P. Eggarter, *Phys. Rev. B* **6**:3598 (1972).
21. F. Dyson, *Phys. Rev.* **92**:1331 (1953).
22. S. N. Evangelou, *J. Phys. C* **19**:4291 (1986); *J. Condensed Matter* **2**:2953 (1990).
23. A. B. Harris, *Phys. Rev. B* **27**:1397 (1985).
24. S. A. Molcanov, *Commun. Math. Phys.* **78**:429 (1981).
25. S. N. Evangelou and E. N. Economou, *Phys. Lett. A* **151**:345 (1990).
26. G. Casati, L. Molinary, and F. Israilev, *Phys. Rev. Lett.* **64**:1851 (1990).